SUPPLEMENTARY FIGURES

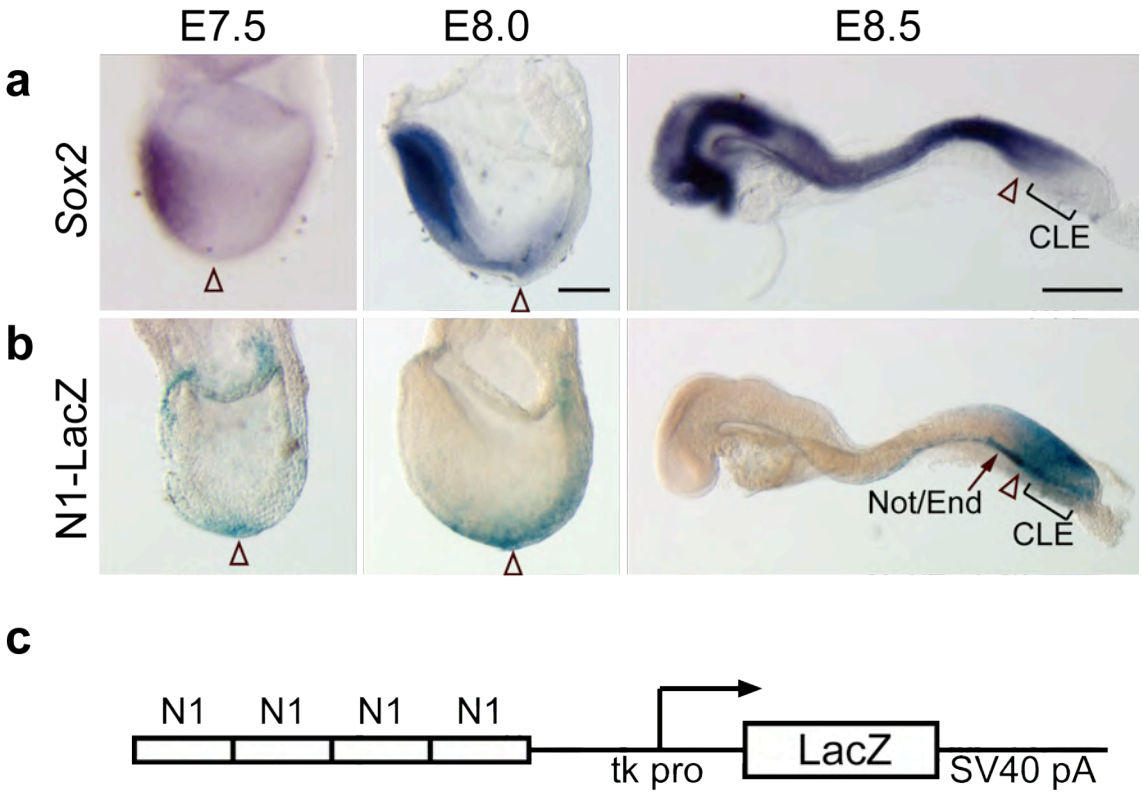

Supplementary Figure 1. Comparison of *Sox2* expression and enhancer N1-LacZ transgene expression in gastrulating mouse embryos. a, b. Comparison of expression patterns of *Sox2* and N1-*LacZ* transgene using stage-matched embryos. N1-LacZ was active in the CLE, node (arrowhead), node-derived notochord (Not) and endoderm (End), while *Sox2* expression was absent in the CLE. **c.** Transgene construct of N1-LacZ. Tetrameric mouse N1 enhancer (301 bp) was inserted in ptkLacZpA upstream of the transcriptional unit consisting of tk promoter, LacZ coding sequence and SV40 polyadenylation signal sequence. Two transgenic mouse lines as well as many primary transgenic embryos were produced, which gave essentially the same expression pattern of LacZ as **b**.

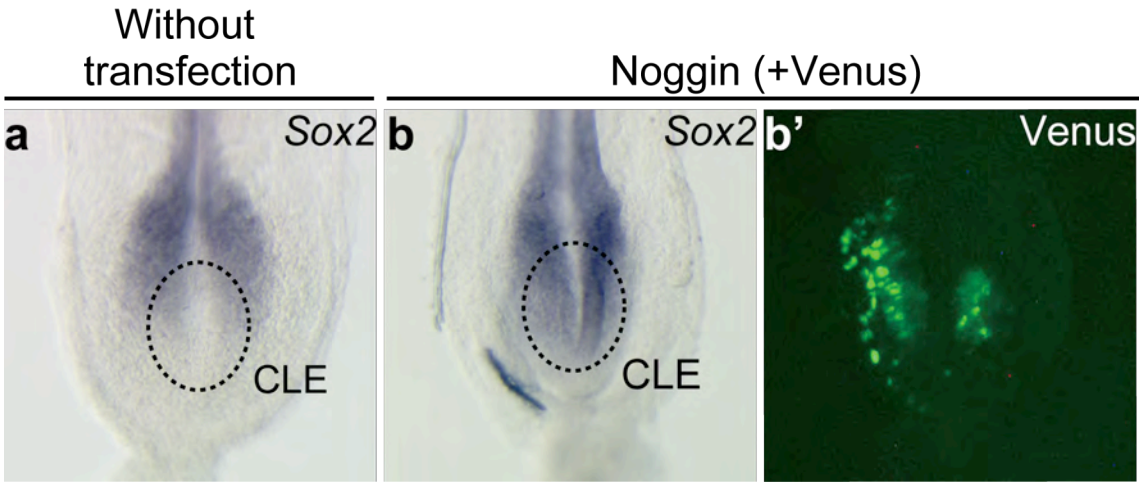

Supplementary Figure 2. Precocious activation of *Sox2* expression in the CLE in embryos transfected with an expression vector for a BMP inhibitor. Embryos in culture were transfected at E8 with a mixture of pCAGGS-cNoggin[4] and pCAGGS-Venus to label transfected cells in the mesoderm lateral to the primitive streak at E8, using the method described by Yamamoto et al.[37] At E8.5, embryos were fixed, the Venus fluorescence recorded (**b'**) and *Sox2* expression examined by in situ hybridization (**b**) and compared with untransfected control embryos (**a**). Note that *Sox2* expression was initiated in the CLE by Noggin expression (**b**), which was absent in the normal embryo (**a**).

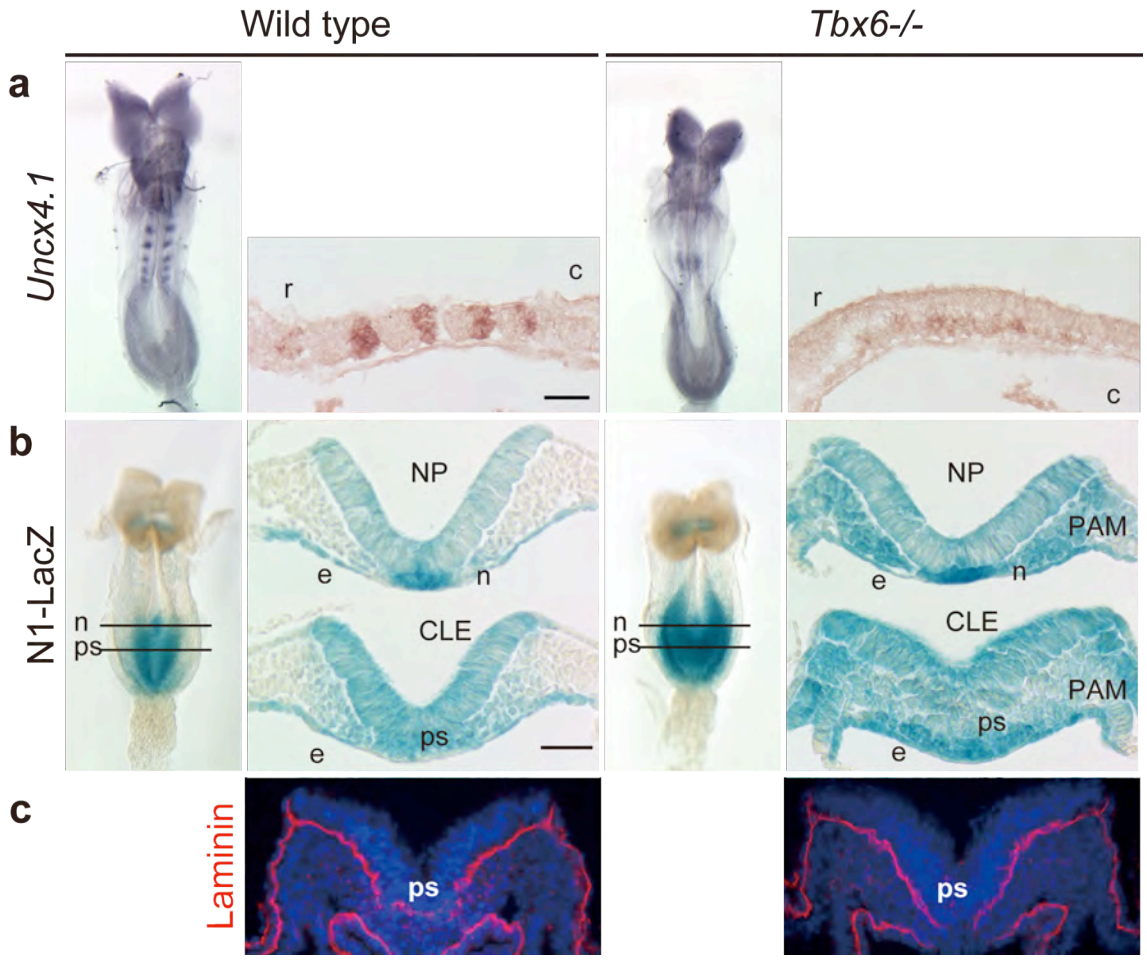

Supplementary Figure 3. Characterization of *Tbx6* mutant embryos.
a. Comparison of *Uncx4.1* expression in wild type and *Tbx6-/-* embryos at E8.5 in whole mount specimens (left panel) and parasagittal sections (right panel). *Uncx4.1* is expressed in the caudal part of segmented somites in wild type, but is largely missing from *Tbx6-/-* embryos. r, rostral; c, caudal. **b.** Activity of enhancer N1 detected by the expression of the N1-LacZ transgene in wild type and *Tbx6-/-* embryos, respectively. Labels are in accordance with Fig. 2. **c.** Laminin immunostaining showing the basal lamina. In both wild type and *Tbx6-/-* embryos, interruption of the basal lamina is confined to the primitive streak region. Scale bars, 50 μm.

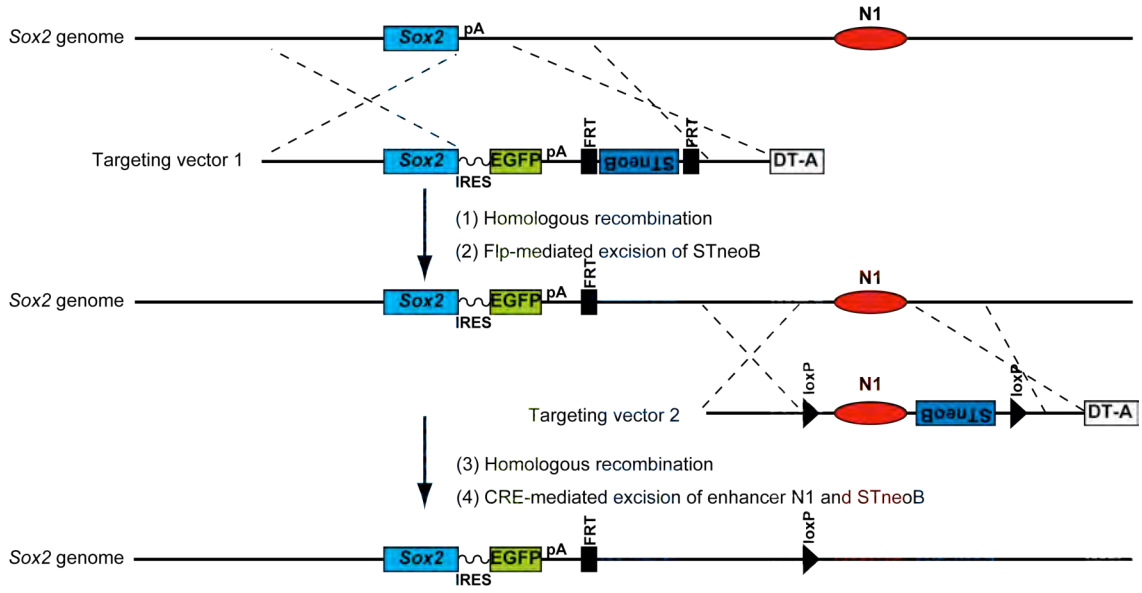

Supplementary Figure 4. A schematic of the production of enhancer N1 mutant mice.

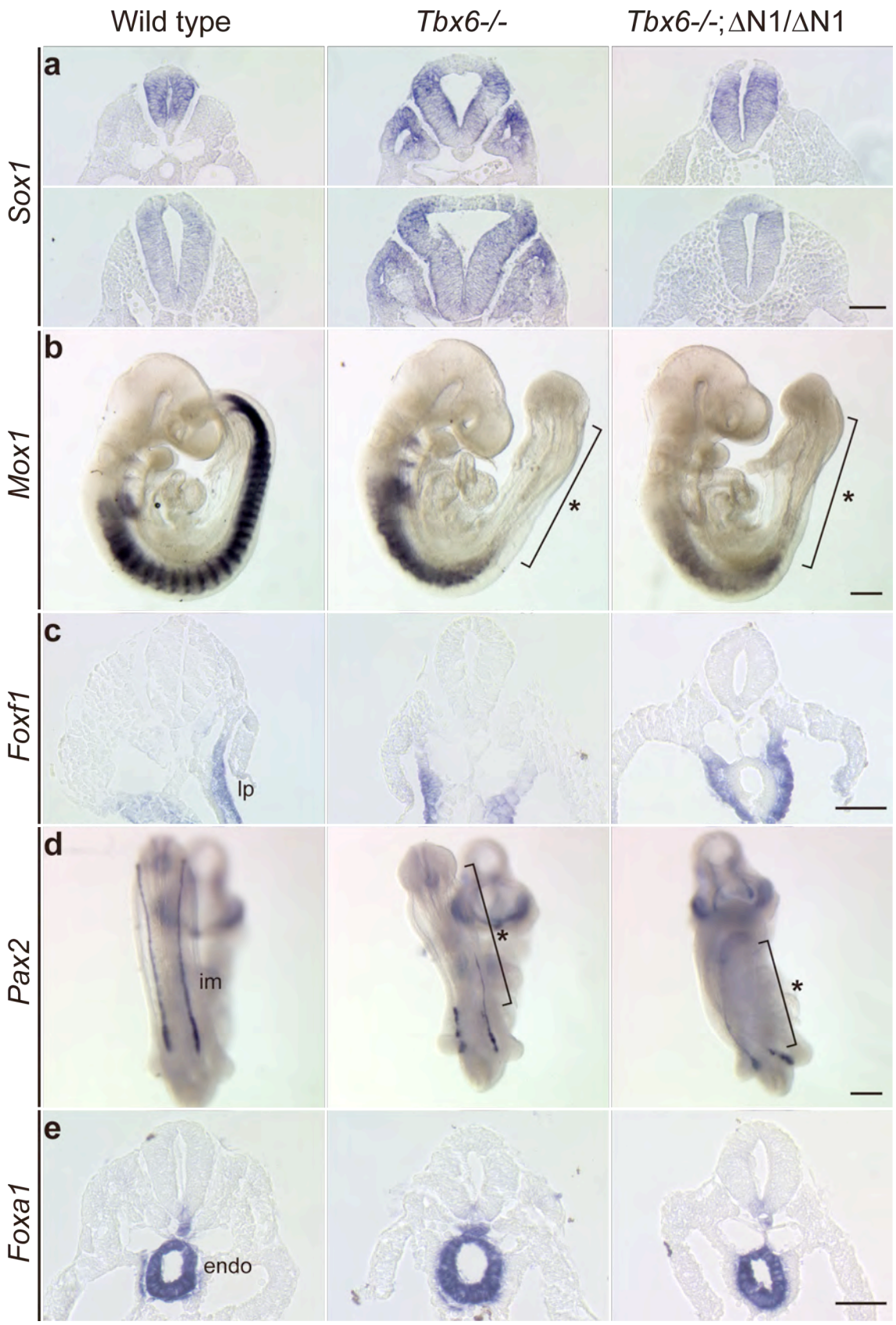
Wild type
Tbx6-/-
Tbx6-/-;ΔN1/ΔN1
Sox1
Mox1
Foxf1
Pax2
Foxa1
a
b
c
d
e
lp
im
endo
*
*
*
*

Supplementary Figure 5. The loss of the neural tube character of the paraxial tissue found in *Tbx6*-/- embryos with the enhancer N1 mutation does not lead to activation of mesoderm or endoderm markers. Wild type, *Tbx6*-/-, and *Tbx6*-/-;ΔN1/ΔN1 embryos at E9.5 were hybridized with probes for *Sox1* (neural), *Mox1* (mesodermal), *Foxf1* (visceral lateral plate (lp)), *Pax2* (intermediate mesoderm (im)) and *Foxa1* (endoderm, (endo)). Sections at a trunk level (**a**, **c**, **e**) or whole mount specimens (**b**, **d**) are shown. The loss of *Mox1* expression in the paraxial mesoderm and *Pax2* in the intermediate mesoderm in the posterior domain of embryos, indicated by asterisks is characteristic of *Tbx6*-/- embryos, and was unaffected in *Tbx6*-/-;ΔN1/ΔN1 double mutants. Scale bars, 50 μm for **a**, **c**, **e** and 300 μm for **b**, **d**.

a

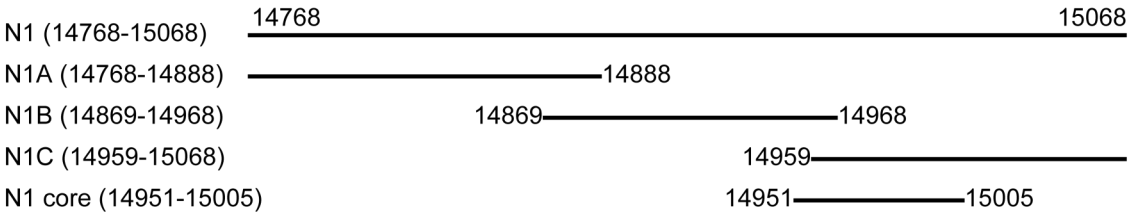

b T-box binding sequence and its mutant

Dimer A	TTTCACACCT-AGGTGTGAAA
Dimer A Mut	TTTGGGACCT-AGGTCCCAAA
Dimer B	TCAGGTGTGAAATT-AATTTCACACCTTG
Dimer B Mut	TCAGGTCCCAAATT-AATTTGGGACCTTG
Monomer	TCAGGTGTGAAATT
Monomer Mut	TCAGGTCCCAAATT

Mesp2 enhancer sequences with T-box binding motifs (Site B and D)

Site B:	CCTTCGAGGGGTCAGAATCCACACCTCTGCAAATGGGCCCGCTTT
mB1:	CCTTCGAGGGGTCAGAATCGATATCTCTGCAAATGGGCCCGCTTT
mB2:	CCTTCGAGAGTACTGAATCCACACCTCTGCAAATGGGCCCGCTTT
Site D:	AACCTGGCAGGGACCCCACCTCACACCTTTAGTCCAGATAAAGCT
mD:	AACCTGGCAGGGACCCCACCTCGCGACTTTAGTCCAGATAAAGCT

c

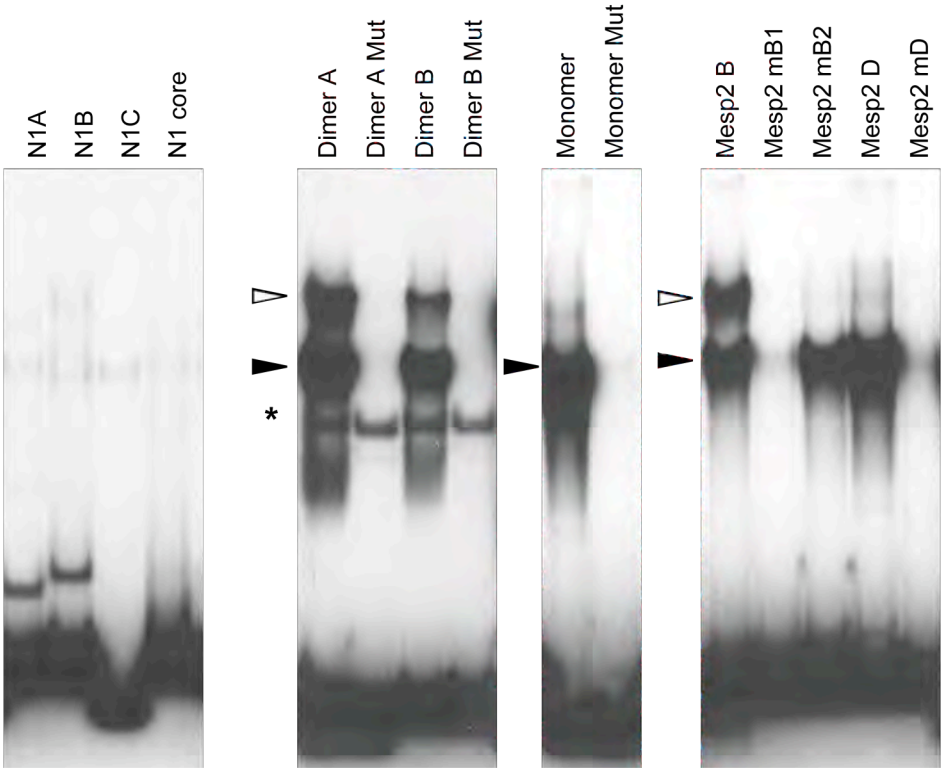

Supplementary Figure 6. Absence of the direct interaction of Tbx6 with the enhancer N1 sequence, as indicated by EMSA. a. Overlapping fragments of enhancer N-1 used as probes. The genomic positions are in accordance with **Fig. 2**. **b.** The established T-box binding sequences and their mutations used for the EMSA analysis. Top: A collection of typical T-box binding sequences selected from random sequences[42,43]. Dimer A, the sequence carrying two T-box binding motifs (red) in convergent arrangement and its mutant version (Dimer A Mut), where the base alterations are indicated in blue. Dimer B, the sequence with divergently arranged two T-box binding motifs and its mutant version (Dimer B Mut). Monomer, the sequence with a singlet T-box binding motif and its mutant version (Monomer Mut). Bottom: Two regions of Mesp2 enhancer sequences with T-box binding motifs to which Tbx6 binding has been demonstrated[15]. Site B, the sequence with divergent-type dimer binding motifs, and its mutated sequences (mB1 and mB2). Site D, the sequence with a singlet T-box binding motif, and its mutated sequence (mD). c. EMSA analysis showing the absence of Tbx6 binding to the enhancer N1 sequence, under the condition where all known T-box binding sequences shown in B were specifically bound by Tbx6. The results using the *Mesp2* enhancer sequence were essentially identical to the previous report[15]. Positions of the probes bound by monomer and dimer of Tbx6 are indicated by solid and open arrowheads, respectively. The asterisk is a non-specific band.

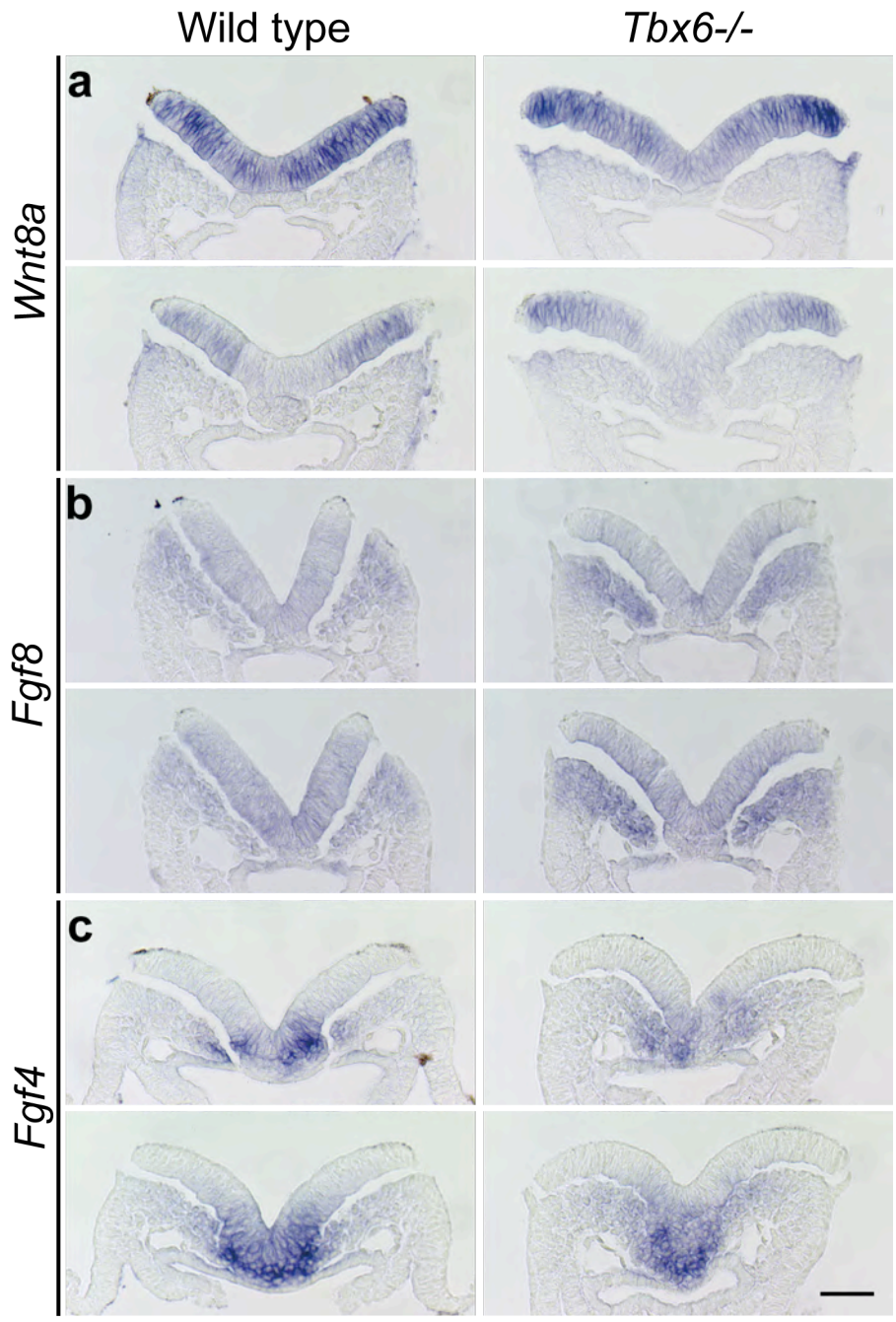

Supplementary Figure 7. Expression of *Wnt8a*, *Fgf8* and *Fgf4* at E8.5 are unaffected in *Tbx6*-/- embryos. Sections at two axial levels around the node of wild type and *Tbx6-/-* embryos are compared after hybridization with respective probes. Scale bar, 50 μm.